

Original Article

DOI 10.1007/s12206-021-0722-x

Keywords:

- Topology optimization
- Multi working conditions
- Unsymmetrical complex plate and shell structures
- Secondary optimization

Correspondence to:

Yixiao Qin
1983015@tyust.edu.cn

Citation:

Zhang, Y., Qin, Y., Gu, J., Jiao, Q., Wang, F., Guo, Z., Zhang, H., Wang, J., Mi, C., Zheng, H. (2021). Topology optimization of unsymmetrical complex plate and shell structures bearing multicondition overload. *Journal of Mechanical Science and Technology* 35 (8) (2021) 3497~3506. <http://doi.org/10.1007/s12206-021-0722-x>

Received November 27th, 2020

Revised March 20th, 2021

Accepted April 29th, 2021

† Recommended by Editor
Hyun-Gyu Kim

Topology optimization of unsymmetrical complex plate and shell structures bearing multicondition overload

Yangyang Zhang¹, Yixiao Qin¹, Jinpeng Gu¹, Qianqian Jiao¹, Feng Wang¹, Zhenshan Guo¹, Hao Zhang¹, Jianjun Wang², Chenghong Mi² and Huaipeng Zheng²

¹College of Mechanical Engineering, Taiyuan University of Science and Technology, Taiyuan 030024, China, ²Xuzhou Construction Machinery Co. Ltd, Xuzhou 221000, China

Abstract Unsymmetrical complex plate and shell structure is one of the common engineering structures. In practice, more redundant materials exist because of the irrationality of this kind of structure with heavy load and multiple working conditions, and the study of its topology optimization has become an engaging topic. Using the SIMP model, topological results show that one side of the main web is a hollow structure, and the other side of the auxiliary web is a truss structure. According to the topological results and considering manufacturable processing, a new structure is redesigned, the size and shape of the redesigned structure is secondary optimized, and the final structure is obtained. The method in this paper not only meets the performance requirements of the unsymmetrical complex plate and shell structures, but also realizes the topology and lightweight. The effectiveness scientific research value of the proposed method is verified by engineering examples.

1. Introduction

Unsymmetrical complex plate and shell structures are widely used in mechanical structures, which makes the effective utilization of materials become the current research hotspot and difficulty [1]. The optimal design of this structure can give full play to the maximum performance of materials and avoid waste of materials. When the structure pursues safety margin subjectively, it often leads to unreasonable design, which will lead to heavy structure and material waste.

The optimal distribution of materials that can be found through topology optimization and then redesigned according to the actual engineering design, processing technology, and structural characteristics can be more conducive to the ideal structure design.

Topology optimization is an efficient method to find the best distribution position of materials. For topology optimization of continuum structure, the number, shape, and distribution location of holes within the design range is mainly determined. The first homogenization method is the beginning of continuous structure topology optimization. Then, the mathematical models of topology optimization such as evolutionary structure optimization, artificial materials, and SIMP [2-4] are proposed successively. The SIMP method is simple in form and widely used; its idea is to introduce a penalty factor to make the intermediate density closer to 0 or 1. In Ref. [5], simultaneous size, shape, and topology optimization of planar and space truss is investigated. Ref. [6] deals with the method for the determination of relations among geometric parameters to reach the optimal shape of the cross section, and the method is based on Lagrange's multipliers used for the determination of extreme values. In Ref. [7], SIMP and gradient level setting methods are compared. Ref. [8] proposes a hybrid method, which combines simulated annealing with the SIMP method to remove medium density elements gradually. Ref. [9] presents the optimization procedure of the extended BESO method and a series of numerical examples in 2D and 3D to demonstrate the effectiveness and efficiency of the proposed approach. Fast lightweight design meets the current market demand, and topology optimization is widely

used in many fields, which is a reliable, convenient method [10].

In the existing research, the optimization object is only for a single web, without considering the constraints of the main web and auxiliary web under the actual main girder condition; hence, the optimization has certain limitations. In this paper, using the mathematical model of SIMP in classical condition considering girder web stress, topology optimization is carried out on the main web and auxiliary web according to the result of topology optimization and considering the fabrication procedure, structure characteristics, and overall aesthetics to produce again to design a kind of unsymmetrical complex plate. Moreover, web member composite structure is redesigned, which combines hollow plate and shell structure with truss structure. This combination of plates and web member meets the requirements of the original performance, reduces unnecessary material waste, and achieves greater material utilization compared with conventional size optimizations with fixed shapes. The method presented in this paper is a novel method for complex structure design, which can optimize the topology of webs with inconsistent forces and make them manufacturable. It makes up for the shortcomings in the design of unsymmetrical complex plate and shell structures, and has an important enlightening effect on the study of unsymmetrical structures and load-bearing structures as well as large-span spatial structures.

2. Mathematical model and constraint conditions for topology optimization of unsymmetrical complex plate and shell structures

2.1 Topology optimization modeling

In the topology optimization research of unsymmetrical complex plate and shell structure, the most common methods are homogenization method for optimization, variable density method, and variable thickness method [11]. The variable density method regards the material as having a variable density, namely, the density is the design variable, the unit material is retained when the density is 1, the element material is deleted when the density is 0, the relative density (0,1) affects the material properties, and a functional relationship exists between the two. A penalty factor is added to make the design variable value close to 0 and 1 because the density between 0 and 1 is difficult to judge whether the material is deleted; thus, the optimal material distribution can be obtained clearly. SIMP introduces a kind of material with a density of 0-1. A nonlinear relationship exists between the density of the design variables and the material. The choice is decided by whether the design variable of the element is 0 or 1 and the element with a penalty factor constraint between 0 and 1. Under a certain material volume, the optimal material distribution of the minimum compliance, that is, the maximum stiffness of the structure, is solved.

The SIMP material interpolation model takes the material compliance as the objective function by constraining the vol-

ume. The mathematical model is as follows:

$$\begin{cases} \mathbf{X} = (x_1 \ x_2 \ \cdots \ x_e \ \cdots \ x_N)^T \in R \\ E = (x_e)^p E_0 \\ p > 1 \\ C(\mathbf{X}) = \mathbf{F}^T \mathbf{U} = \mathbf{U}^T \mathbf{K} \mathbf{U} = \sum_{e=1}^N (x_e)^p \mathbf{u}_e^T \mathbf{k}_0 \mathbf{u}_e \\ V = fV_0 = \sum_{e=1}^N x_e v_e \\ 0 < x_{\min} \leq x_e \leq x_{\max} \leq 1 \end{cases} \quad (1)$$

where \mathbf{X} is the design variable, also known as the relative density; x_e is the relative density of the unit; E is the equivalent elastic modulus of the material; E_0 is the original elastic modulus of the material; p is the penalty factor; C is the structural compliance; \mathbf{F} is the external force vector of the structure; \mathbf{U} is the displacement vector of the structure; \mathbf{K} is the stiffness matrix of the structure; \mathbf{u}_e is the displacement column vector of the material element; \mathbf{k}_0 is the element stiffness matrix; f is the optimized ratio of the material volume; V_0 is the initial volume of the design domain; V is the volume of the optimized structure; v_e is the unit volume; x_{\min} and x_{\max} are the minimum and maximum limits of the relative density of the element. The purpose of introducing x_{\min} is to prevent the singularity of element stiffness matrix.

The mathematical model of SIMP interpolation method is the Lagrange multiplier method. The Lagrange function of the topology optimization mathematical model is obtained as follows:

$$\begin{aligned} L(x_e) = & C(x_e) + \lambda_1^T (\mathbf{K} \mathbf{U} - \mathbf{F}) + \lambda_2 (V - fV_0) \\ & + \sum_{e=1}^N \lambda_3 (x_{\min} - x_e + a_e^2) \\ & + \sum_{e=1}^N \lambda_4 (x_e - x_{\max} + b_e^2) \end{aligned} \quad (2)$$

where λ_1 , λ_2 , λ_3 , and λ_4 are Lagrange multipliers, and a_e , b_e is the relaxation factor. When variable x_e is at extreme point x^* , the mathematical model of topology optimization based on the SIMP interpolation satisfies the following Kuhn-Tucker conditions:

$$\begin{cases} \frac{\partial L(x_e)}{\partial x_e} = \frac{\partial C(x_e)}{\partial x_e} + \lambda_1^T \frac{\partial (\mathbf{K} \mathbf{U} - \mathbf{F})}{\partial x_e} \\ \quad + \lambda_2 \frac{\partial (V - fV_0)}{\partial x_e} - \lambda_3 + \lambda_4 = 0 \\ V = fV_0 \\ \mathbf{F} = \mathbf{K} \mathbf{U} \\ \lambda_3 (x_{\min} - x_e) = 0 \\ \lambda_4 (x_e - x_{\max}) = 0 \\ \lambda_1, \lambda_2, \lambda_3, \lambda_4 \geq 0 \\ 0 < x_{\min} \leq x_e \leq x_{\max} \leq 1 \end{cases} \quad (3)$$

Table 1. Structural parameters of deflection rail beam of 300 t casting crane.

Main girder height (mm)	Thickness of upper flange plate (mm)	Thickness of lower flange plate (mm)	Thickness of main web (mm)	Thickness of auxiliary web (mm)	Width of upper flange plate (mm)	Width of lower flange plate (mm)
3000	20	20	14	10	2185	2020

According to the Kuhn-Tucker condition, the following formula is obtained:

$$B_e^k = \frac{x_e^{k+1}}{x_e^k} = \frac{U^T \frac{\partial K}{\partial x_e} U}{\lambda_2 \frac{\partial V}{\partial x_e}} = \frac{p(x_e)^{p-1} u_e^T k_0 u_e}{\lambda_2 v_e}. \quad (4)$$

The iterative formula based on the optimization criterion method is as follows:

$$x_e^{k+1} = \begin{cases} (B_e^k)^\delta x_e^k & x_{\min} < (B_e^k)^\delta x_e^k < x_{\max} \\ x_{\min} & (B_e^k)^\delta x_e^k < x_{\min} \\ x_{\max} & (B_e^k)^\delta x_e^k > x_{\max} \end{cases} \quad (5)$$

where k is the iteration algebra, and δ is the damping coefficient, which ensures the stability and convergence of the numerical calculation.

2.2 Constraint conditions of strength and stiffness optimization for finite element modeling and analysis of unsymmetrical complex plate and shell structures

In this paper, the main girder of 300/140 t-28 m casting crane is taken as the research object of the unsymmetrical complex plate shell structure. The material is Q345 steel, and the safety factor is 1.48. When $\sigma_s/\sigma_b \geq 0.7$, the basic allowable stress of steel is as follows:

$$[\sigma] = \frac{0.5\sigma_s + 0.35\sigma_b}{1.48} = \frac{0.5 \times 345 + 0.35 \times 470}{1.48} = 227.7 \text{ MPa} \quad (6)$$

where σ_s is the yield point of steel, its unit is MPa; σ_b is the tensile strength of steel, its unit is MPa.

When the crane is in the mid span position, the allowable vertical static deflection is as follows:

$$[Y_s] = \frac{S}{750} = \frac{28000}{750} = 37.3 \text{ mm} \quad (7)$$

where S is the span length of main girder.

When analyzing the stress and deflection of the dangerous

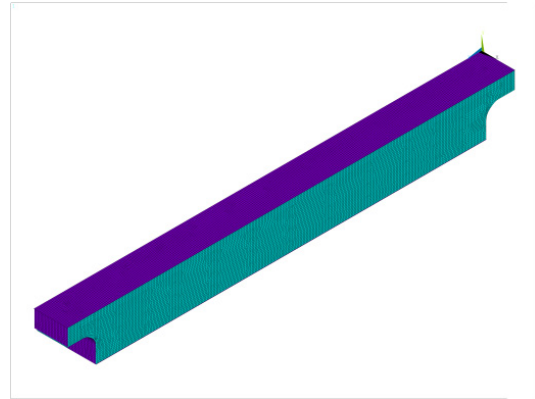


Fig. 1. Model of unsymmetrical complex plate and shell structure.

point of the structure, as shown in Fig. 1, shell63 element is selected to model the single girder. The X-axis direction is the girder width direction, the Y-axis direction is the girder height direction, and the Z-axis direction is the girder length direction.

The structural parameters of unsymmetrical plate welded girder are shown in Table 1.

According to the working environment and actual working condition of casting crane [12], UX, UY, and UZ translational degrees of freedom and ROTZ and ROTY rotational degrees of freedom are imposed on the end of one side of the main girder. The end of the other side is constrained by ROTZ and ROTY rotational degrees of freedom and UX and UY translational degrees of freedom. Gravity degree of freedom $g = 9.81 \text{ m/s}^2$. The wheel pressure of the trolley is applied to the four wheels of the track by uniform force distribution. Three working conditions are considered, that is, the trolley runs with full load to the middle span, left end, and right end of main girder.

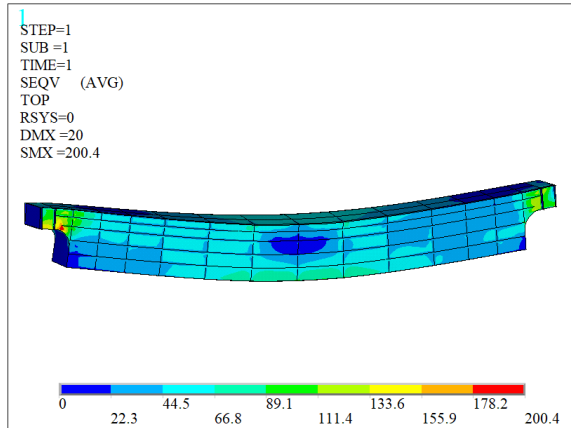
The analysis results of three different working conditions are shown in Fig. 2, and the maximum stress and maximum deflection are shown in Table 2.

Finite element analysis shows that the maximum normal stress of the main girder under three different working conditions is 200.4 MPa, which is less than the allowable stress and meets the requirements of static strength. Moreover, when the full load of the trolley is located at the middle of the span, the maximum displacement in the Y direction is 20.0 mm, which is less than the allowable vertical static stiffness. The crane meets the design specification.

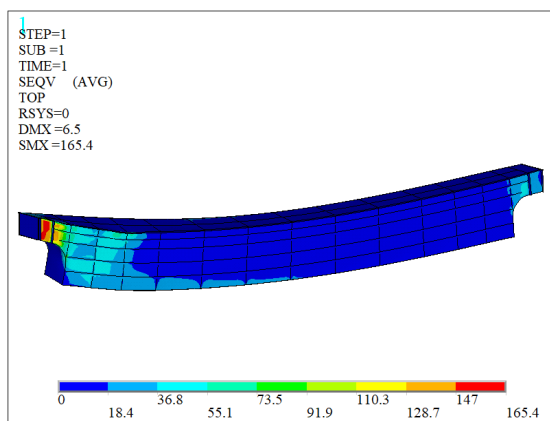
The stress nephogram shows that the stress in most areas of the web of the main girder is not large, much less than the allowable stress; thus, the web material has a surplus, and the web needs to be optimized.

Table 2. Maximum stress and maximum deflection at different positions.

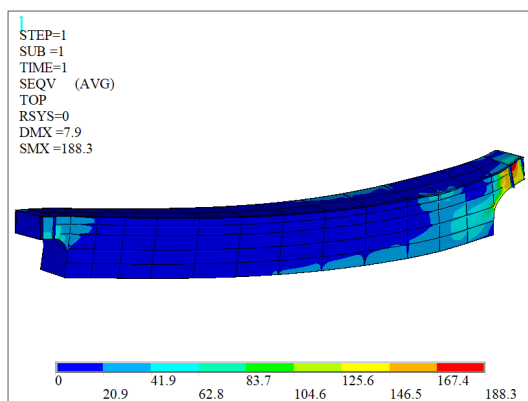
Full load position	Mid span	Left end	Right end
Maximum stress (Mpa)	200.4	165.4	188.3
Maximum deflection (mm)	20.0	6.5	7.9



(a)



(b)



(c)

Fig. 2. Analysis results of three different working conditions: (a) analysis results with load at midspan; (b) analysis results with load at left end; (c) analysis results with load at right end.

3. Topology optimization of unsymmetrical complex plate and shell structures

3.1 Topology optimization of the web

Topology optimization can be realized in two ways: static stiffness optimization and dynamic frequency optimization. With the mathematical model of SIMP [13, 14], the topology optimization of static stiffness under various working conditions is carried out. The element density of the main and auxiliary webs of the main girder is set as the design variables, and topology optimization is carried out by using the optimization criterion method. The convergence speed of the optimization criterion method is fast, and the reciprocal information is not used in the calculation. It is suitable for the problem optimization under single-constraint conditions. The optimization is as follows:

1) The optimization area is set as unit 1, and the area that does not need to be optimized is set as the unit larger than 1. The web of the main girder is set as No. 1 element, and others are set as non 1 element because only shell93 can be used for topology optimization. The loads of the trolley at the middle span, left end, and right end are loaded.

2) The optimization function is defined as the combined compliance considering various working conditions, and the objective function is the overall compliance of the main girder. Taking the volume of the main girder web as constraints, 30 %, 40 %, and 50 % of the volume are constrained, and the optimization accuracy is 0.0001.

3) The number of iterations is set to 30.

4) The topology optimization results with three constraints are obtained and compared.

3.2 Topology optimization results

When 30 % volume is omitted, the main web of the main girder begins to appear void, and the auxiliary web appears similar to the truss structure.

When 40 % of the volume is omitted, the area deleted by the main web of the main girder continues to grow, while the auxiliary web continues to present an evident truss structure.

When 50 % of the volume is omitted, the main web of the main girder is a hollow structure, and the auxiliary web is a truss structure.

The volume is set as a constraint, and 30 %, 40 %, and 50 % are saved for topology analysis. The topology analysis results are shown in Figs. 3-5 and Table 3. The concept diagram of a new type of unsymmetrical complex plate and shell structure is obtained. When the restraint volume is 50 %, the maximum deflection of the web is 34.4 mm. It is the closest to the allowable maximum deflection. The topological result diagram shows that the main web has a hollow web structure, and the auxiliary web has an apparent truss structure, which provides a design idea for the main beam design of a new type of unsymmetrical complex plate and shell structure [15]. The relationship between the compliance of the objective function and

the number of iterations is shown in Figs. 6-8.

4. Regularization design after topology optimization

According to the mathematical model of the SIMP in the third section of the web topology optimization, according to the optimization results and comprehensive consideration of processing technology, structural characteristics and the overall aesthetics of the web to be processed again. Figs. 3-5 show that the middle part of the material on the main web is removed, and the material distribution of the auxiliary web presents a truss structure. It is redesigned according to the processing

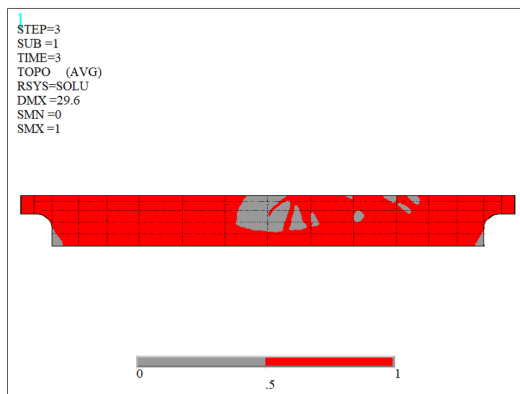
technology, as shown in Fig. 9. On the side of the main web, a vierendeel plate structure is used. The initial size of the opening hole is 1000 mm wide and 1500 mm high, and the radius of the round hole is 450 mm. A truss structure is used on the side of the auxiliary web. Each truss is connected through the joint between the baffle and the flange plate. The diameter of the web member is initially set at 50 mm.

4.1 Secondary optimization of the new complex plate and shell structure

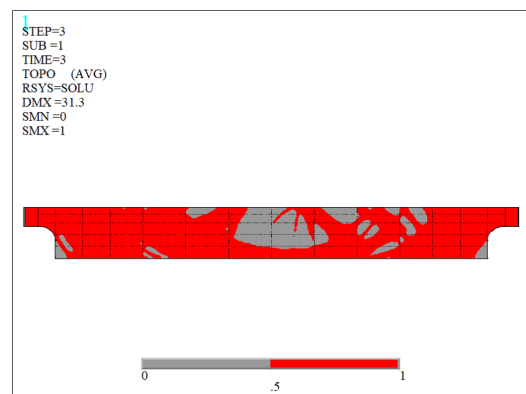
The hole height and width of open main web and the radius of truss structural members are set as design variables. As the

Table 3. Topology optimization parameters and results.

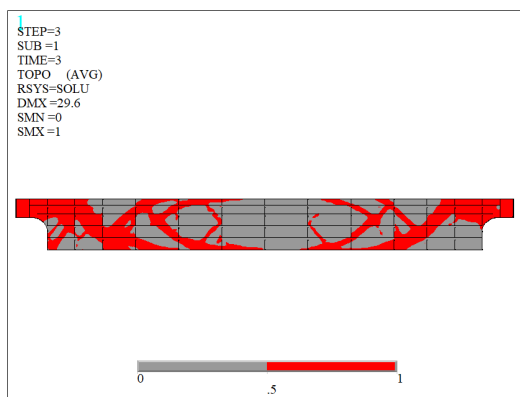
Optimization of regional	Unit used	Objective function	Iterations	Precision	Applied load	Volume of constraint	Maximum displacement of main girder after optimization (mm)
Main web auxiliary web	Shell93	Overall compliance of the main girder	30	0.0001	Full load in midspan, left end, and right end	30 %	29.6
						40 %	31.3
						50 %	34.4



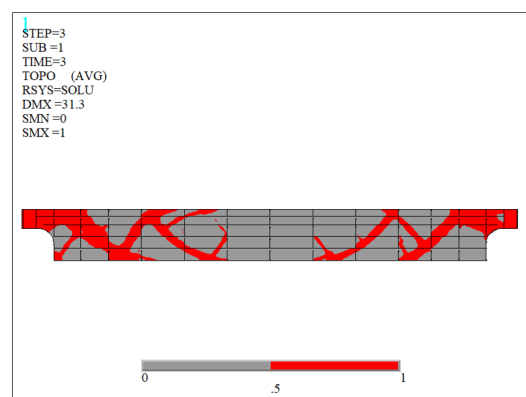
(a)



(a)



(b)



(b)

Fig. 3. Results of topology optimization of web without 30 % volume: (a) results of topology optimization of main web; (b) results of topology optimization of auxiliary web.

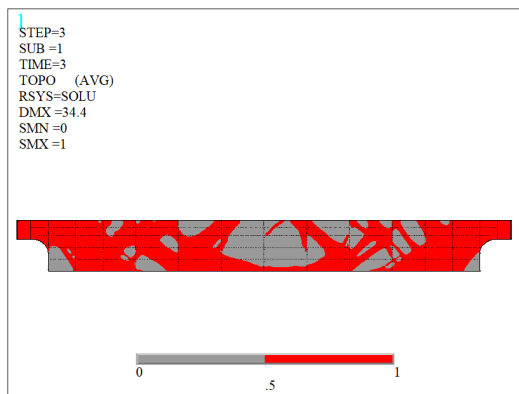
Fig. 4. Results of topology optimization of web without 40 % volume: (a) results of topology optimization of main web; (b) results of topology optimization of auxiliary web.

length direction of the main girder is a symmetrical structure, the optimization variables are shown in Fig. 10, and the remaining holes are symmetrically distributed with the midspan as the center line. The maximum deflection and maximum stress of the main beam are set as constraints, and the total volume is set as the objective function. By using the method of function approximation, the sizes of the holes and truss are found when the minimum volume under allowable deflection and allowable stress is found.

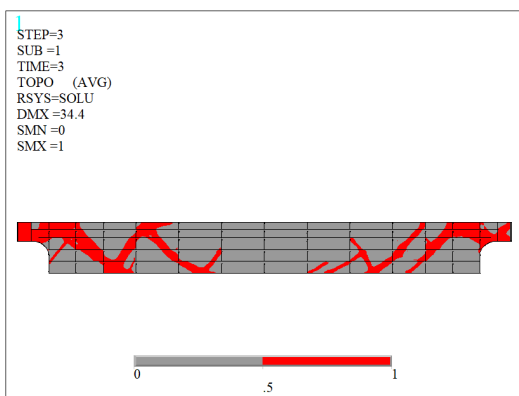
Fig. 11 shows the relationship between objective function (volume) and number of iterations. After 20 times, the iteration volume tends to converge. Table 4 shows the values of variables before and after design. The optimized model is shown in Fig. 12.

4.2 Finite element analysis of a new type of unsymmetrical complex plate and shell structure

The new unsymmetrical complex plate shell structure is analyzed under the same three working conditions, as shown in Fig. 13, and the maximum stress and maximum deflection are



(a)



(b)

Fig. 5. Results of topology optimization of web without 50 % volume: (a) results of topology optimization of main web; (b) results of topology optimization of auxiliary web.

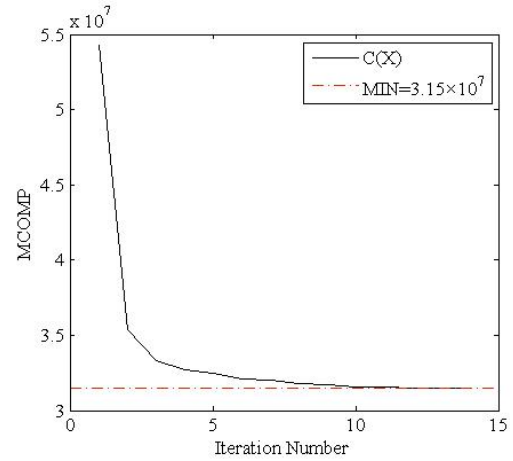


Fig. 6. Relationship between objective function and iteration number without 30 % volume.

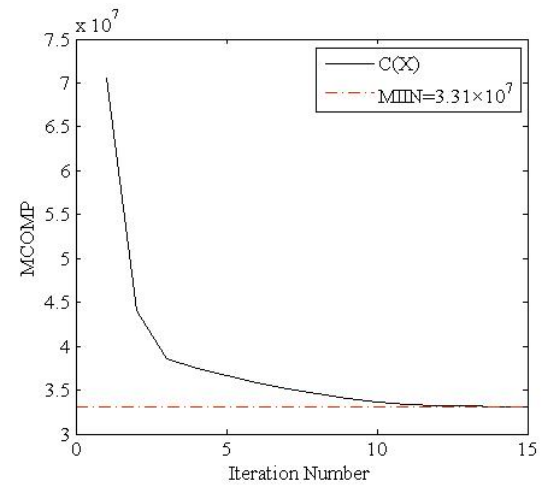


Fig. 7. Relationship between objective function and iteration number without 40 % volume.

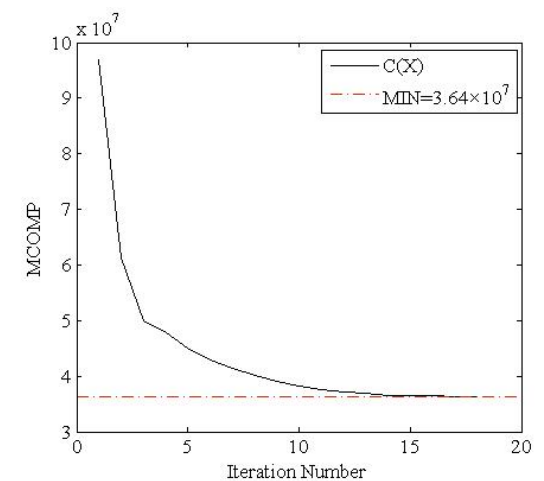


Fig. 8. Relationship between objective function and iteration number without 50 % volume.

shown in Table 5.

According to the finite element analysis, the maximum normal stress of the main girder under three different working conditions is 226.4 MPa, which is less than the allowable stress and meets the requirements of static strength. Moreover, when the full load is located in the middle of the span, the maximum displacement in Y direction is 26.1 mm, which is less than the allowable vertical static stiffness. The crane meets the design specification [16].

Table 4. Comparison of design variables before and after.

	Before optimization (mm)	After optimization (mm)
R_1	50	40
K_1	1000	1150
K_2	1000	940
K_3	1000	1150
K_4	1000	901
K_5	1000	968
G_1	1500	1472
G_2	1500	1565
G_3	1500	1576
G_4	1500	1593
G_5	1500	1413

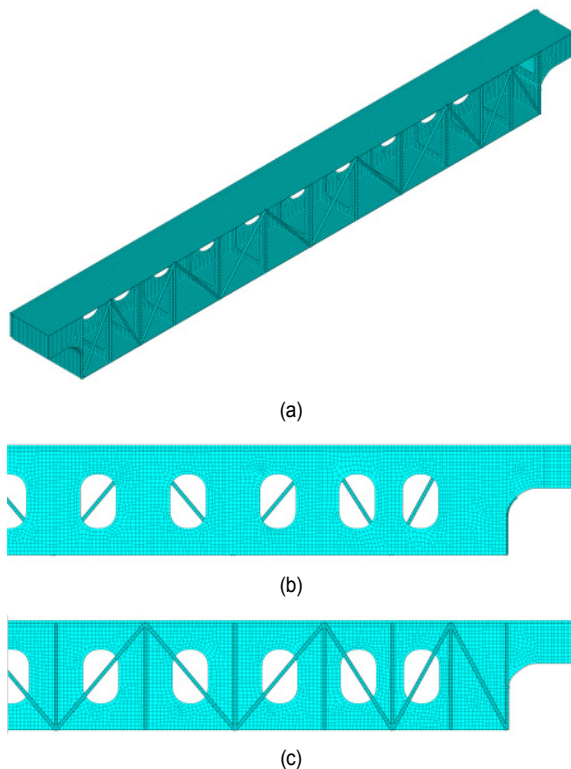


Fig. 9. New unsymmetrical complex plate shell structure model: (a) overall drawing; (b) local detail drawing of main web side; (c) local detail drawing of auxiliary web side.

4.3 Comparative analysis of design results

The analysis of multiple working conditions shows that the maximum stress and maximum disturbance of crane before and after optimization meet the design specification. After optimization [17], the volume and weight decrease by 18 %. Compared with the topology optimization in document [18], the weight of the main girder in this paper is reduced by 5 %, which proves the feasibility and advanced nature of the optimization design.

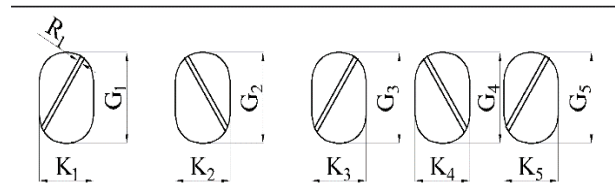


Fig. 10. Design variables.

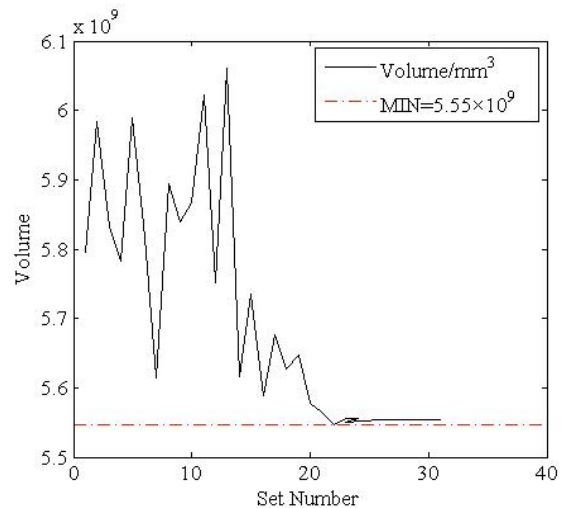


Fig. 11. Relationship between objective function (volume) and set number.

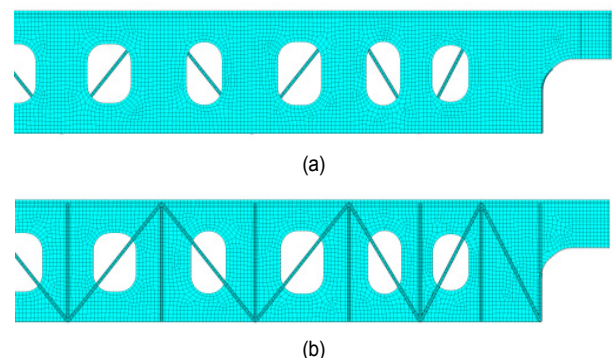
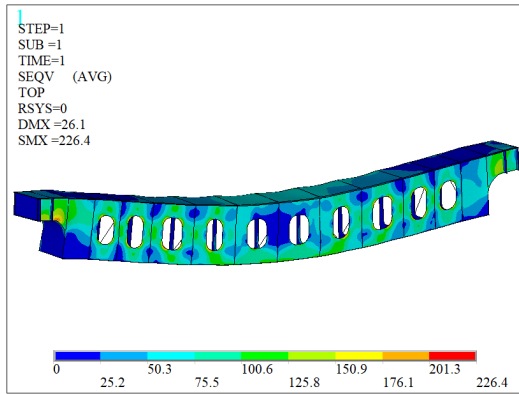


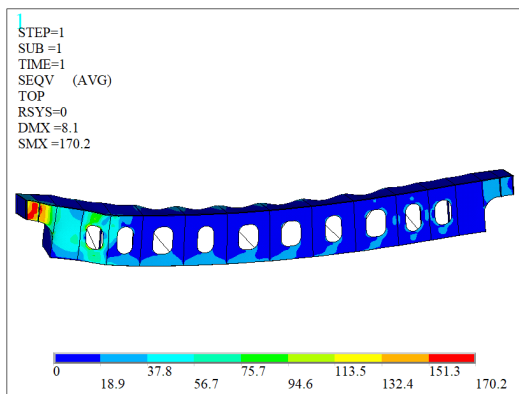
Fig. 12. After secondary optimization of main and auxiliary webs: (a) local detail drawing of main web side; (b) local detail drawing of auxiliary web side.

Table 5. Maximum stress and maximum deflection of full load at different positions after optimization.

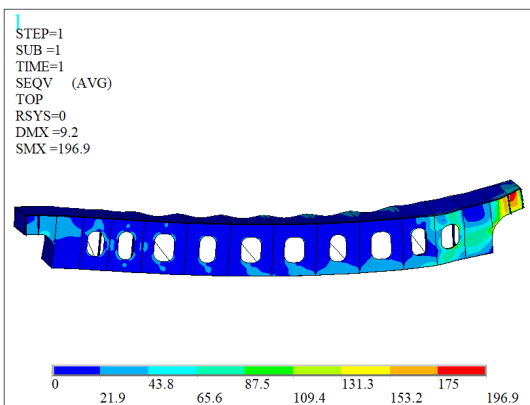
Full load position	Mid span	Left end	Right end
Maximum stress (Mpa)	226.4	170.2	196.9
Maximum displacement (mm)	26.1	8.1	9.2



(a)



(b)



(c)

Fig. 13. Analysis results of three different working conditions after optimization: (a) analysis results of full load in mid span after optimization; (b) analysis results of full load at the left end after optimization; (c) analysis results of full load at the right end after optimization.

Table 6. Maximum stress comparison.

Full load position	Before optimization (Mpa)	After optimization (Mpa)
Mid span	200.4	226.4
Left end	165.4	170.2
Right end	188.3	196.9

Table 7. Maximum disturbance comparison.

Full load position	Before optimization (mm)	After optimization (mm)
Mid span	20.0	26.1
Left end	6.5	8.1
Right end	7.9	9.2

Table 8. Volume, weight, and change rate of unsymmetrical complex plate and shell structure before and after optimization.

Web type	Volume (m ³)	Weight (t)	Rate of change
Before optimization	6.7	52.6	18 %
After optimization	5.5	43.1	

5. Conclusion

1) The variable density interpolation model is simple in form and easy to implement, making it a promising interpolation method. The convergence speed of the optimization criterion method is fast, and it is suitable for the optimization problem of the SIMP interpolation model.

2) The force of the two webs before optimization is inconsistent, but the structure form is symmetrical and the same. This structure form is relatively backward. A performance margin is observed in most positions after finite element analysis, which results in material waste and cost increase.

3) The new type of unsymmetrical complex plate and shell structure is obtained by topology analysis under multiple working conditions. The concept map of topology optimization is obtained and forms the unsymmetrical structure. The main web of the structure uses the hollow structure, and the auxiliary web uses the truss structure. The manufacturability of the structure is designed, and the size is optimized twice. The optimized structure not only meets the requirements of performance but also realizes the rationalization and lightweight of the structure and reduces the manufacturing cost.

Acknowledgments

This work was supported by the 13th Five-Year National Key Research and Development Projects [2017YFC0703906], the Shanxi Provincial Key Research and Development Project [201903D121067], and the Fund for Shanxi "1331Project" Key Subjects Construction [1331KSC].

Nomenclature

X	: Design variable
x_e	: Relative density of the unit
E	: Equivalent elastic modulus of the material
E_0	: Original elastic modulus of the material
p	: Penalty factor
C	: Compliance of the structure
F	: External force vector of the structure
U	: Displacement vector of the structure
K	: Stiffness matrix of the structure
u_e	: Displacement column vector of material element
k_0	: Element stiffness matrix
f	: Optimized ratio of material volume
V_0	: Initial volume of the design domain
V	: Volume of the optimized structure
v_e	: Unit volume
x_{\min}	: Minimum limits of the relative density of the element
x_{\max}	: Maximum limits of the relative density of the element
λ_1	: Lagrange multiplier
λ_2	: Lagrange multiplier
λ_3	: Lagrange multiplier
λ_4	: Lagrange multiplier
a_e	: Relaxation factor
b_e	: Relaxation factor
k	: Iteration algebra
δ	: Damping coefficient
σ_s	: Yield point
σ_b	: Tensile strength
S	: Span length of main girder

References

- [1] D. D. Zhang, Y. Lv, Q. L. Zhao and F. Li, Development of lightweight emergency bridge using GFRP-metal composite plate-truss web, *Engineering Structures*, 196 (109291) (2019) 1-22.
- [2] T. Evangelos and S. Martin, Messing with boundaries - quantifying the potential loss by preset par-ameters in topology optimization, *Procedia CIRP*, 84 (2019) 979-985.
- [3] X. D. Huang, Z. H. Zuo and Y. M. Xie, Evolutionary topological optimization of vibrating continuum structures for natural frequencies, *Computers and Structures*, 88 (5-6) (2010) 357-364.
- [4] R. Ortigosa, D. Ruiz and A. J. Gil, A stabilisation approach for topology optimisation of hyperelastic structures with the SIMP method, *Computer Methods in Applied Mechanics and Engineering*, 364 (112924) (2020) 1-24.
- [5] G. Ghanshyam, J. Vimal, K. Vivek and P. V. Savsani, Size, shape, and topology optimization of planar and space trusses using mutation-based improved metaheuristics, *Journal of Computational Design and Engineering*, 5 (2) (2018) 198-214.
- [6] M. Milomir, M. Mile and R. Radovan, Optimization of a pentagonal cross section of the truck crane boom using Lagrange's multipliers and differential evolution algorithm, *Mechanica*, 46 (2011) 845-853.
- [7] G. David, W. William and F. Mohamed, High-resolution non-gradient topology optimization, *Journal of Computational Physics*, 372 (2018) 107-125.
- [8] N. P. Garcia-Lopez, M. Sanchez-Silva and A. L. Medaglia, A hybrid topology optimization methodology combining simulated annealing and SIMP, *Computers and Structures*, 89 (15-16) (2011) 1512-1522.
- [9] B. Xu, L. Zhao, W. Y. Li, J. J. He and Y. M. Xie, Dynamic response reliability based topological optimization of continuum structures involving multi-phase materials, *Composite Structures*, 147 (2016) 134-144.
- [10] J. Davin et al., Developing topology optimization with additive manufacturing constraints in ANSYS®, *IFAC-PapersOnLine*, 51 (11) (2018) 1359-1364.
- [11] R. Christian, F. W. Wang and S. Ole, Buckling strength topology optimization of 2D periodic materials based on linearized bifurcation analysis, *Computer Methods in Applied Mechanics and Engineering*, 339 (2018) 115-136.
- [12] X. W. Wu, B. Chen, D. Zhang and J. Li, The research on optimal design of large metallurgical crane, *Procedia Engineering*, 24 (2011) 783-787.
- [13] X. C. Jiang, H. Wang, Y. Li and K. J. Mo, Machine learning based parameter tuning strategy for MMC based topology optimization, *Advances in Engineering Software*, 149 (102841) (2020) 1-11.
- [14] C. S. Edwards, H. A. Kim and C. J. Budd, An evaluative study on ESO and SIMP for optimising a cantilever tie—beam, *Structural and Multidisciplinary Optimization*, 34 (2007) 403-414.
- [15] H. T. Qiao, S. J. Wang, T. J. Zhao and H. Tang, Topology optimization for lightweight cellular material and structure simultaneously by combining SIMP with BESO, *Journal of Mechanical Science and Technology*, 33 (2019) 729-739.
- [16] A. Li, C. Liu and S. Z. Feng, Topology and thickness optimization of an indenter under stress and stiffness constraints, *Journal of Mechanical Science and Technology*, 32 (2018) 211-222.
- [17] H. P. Panganiban, W. C. Kim, T. J. Chung and G. W. Jang, Optimization of flatbed trailer frame using the ground beam structure approach, *Journal of Mechanical Science and Technology*, 30 (2016) 2083-2091.
- [18] S. Ole and M. Kurt, Topology optimization approaches, *Structural and Multidisciplinary Optimization*, 48 (2013) 1031-1055.



Yangyang Zhang is a graduate student of the Taiyuan University of Science and Technology. His research interests include optimization design of engineering structure and hoisting machinery.



Yixiao Qin is a Professor and Doctoral Supervisor in the Taiyuan University of Science and Technology. He received his Ph.D. degree from the Shanghai Institute of Applied Mathematics and Mechanics. He is a Standards Committee and International fellow. His research interests include optimization design of

engineering structure.



Jinpeng Gu is a Doctor of the Taiyuan University of Science and Technology. His research interests include mechanical vibration and green logistics.